Jour. Fac. Sci., Hokkaido Univ., Ser. VII (Geophysics), Vol. 7, No. 5 401-420, 1985.

Seismic Wave Propagation in a Stratified Half-Space

Tsutomu Sasatani

Department of Geophysics, Faculty of Science, Hokkaido University, Sapporo 060, Japan

(Received October 29, 1984)

Abstract

A simple approach to evaluate the stratified half-space response is proposed. This approach is the combination of the reflection and transmission properties of elastic media (Kennett and Kerry, 1979) with the discrete wavenumber summation method (Bouchon, 1981). Numerical examples show that surface reflected phases play an important role in shaping the nature of the seismograms for local earthquakes.

1. Introduction

The problem of the excitation and propagation of seismic waves in a stratified elastic half-space has been extensively discussed since the pioneering work of Lamb (1904). Recently, many approaches have been proposed to evaluate the response of elastic solid to excitation by transient point sources. For example, there are generalized ray theory (Helmberger, 1968 ; Sato, 1973), reflectivity method (Fuchs and Müller, 1971 ; Kind, 1978), reflection and transmission matrices method (Kennett, 1983 ; Kennett and Kerry, 1979), and discrete wavenumber method (Bouchon, 1979, 1981).

In this paper, we propose a simple approach to evaluate the stratified half-space response. This approach is based on the three-dimensional seismic wavefield of Aki and Richards (1980), the reflection and transmission properties of elastic media of Kennett and Kerry (1979), and the wavenumber integration of Bouchon (1981). Yao and Harkrider (1983) have proposed essentially the same approach. As numerical example, we show the effect of a single surface layer on seismograms for local earthquakes.

2. Three dimensional seismic wavefield

Here we shall follow Aki and Richards (1980; chapter 7) in deriving a complete representation of the three dimensional seismic wavefield.

We consider a cylindrical coordinate system (r, θ, z) in an isotropic elastic medium with stratification perpendicular to the z axis (Fig. 1). The elastic displacement in a homogeneous body can be expressed in terms of the three scalar potentials ϕ, ψ, χ, as

$$\boldsymbol{U} = \nabla\phi + \nabla \times \nabla \times (0, 0, \psi) + \nabla \times (0, 0, \chi). \tag{1}$$

The potentials ϕ, ψ, χ represent P-, SV-, and SH- waves, respectively and satisfy the following wave equations

$$\ddot{\phi} = \alpha^2 \nabla^2 \phi, \quad \ddot{\psi} = \beta^2 \nabla^2 \psi, \quad \ddot{\chi} = \beta^2 \nabla^2 \chi, \tag{2}$$

where α and β are P-wave and S-wave velocities, and overdots are used to indicate time derivatives. The basic solutions to (2) can be obtained by the method of separation of variables. They are, for example,

$$\begin{aligned}
\phi(r, \theta, z; \omega) &= J_m(kr)[\cos m\theta(Ae^{-\gamma z} + Be^{\gamma z}) \\
&\quad + \sin m\theta(A'e^{-\gamma z} + B'e^{\gamma z})] \exp(-i\omega t), \\
\psi(r, \theta, z; \omega) &= J_m(kr)[\cos m\theta(Ce^{-\nu z} + De^{\nu z}) \\
&\quad + \sin m\theta(C'e^{-\nu z} + D'e^{\nu z})] \exp(-i\omega t), \\
\chi(r, \theta, z; \omega) &= J_m(kr)[\cos m\theta(Ee^{-\nu z} + Fe^{\nu z}) \\
&\quad + \sin m\theta(E'e^{-\nu z} + F'e^{\nu z})] \exp(-i\omega t),
\end{aligned} \tag{3}$$

where $J_m(kr)$ is the m th-order Bessel function; k is the horizontal wavenumber; m is an integer; A, A', B, B', $\cdots$, F, F' are constants; $\gamma = (k^2 - \omega^2/\alpha^2)^{1/2}$, Im $\gamma \leq 0$; $\nu = (k^2 - \omega^2/\beta^2)^{1/2}$, Im $\nu \leq 0$; ω is the angular frequency; and t is the time. If we substitute potentials of the form (3) into (1) and the stress-displacement relations, we find that the displacement $\boldsymbol{U}$ and the traction $\boldsymbol{T}(\tau_{rz},$

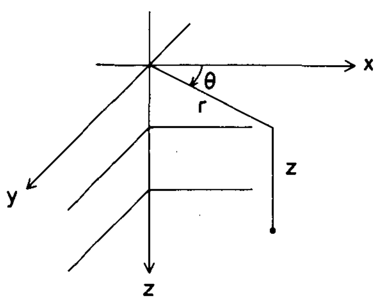

Fig. 1 Orientation of cylindrical polar coordinates used to analyze waves from a point source in a stratified half-space.

$\tau_{z\theta}$, τ_{zz}) acting on the horizontal plane at depth z have the following from

$$\begin{aligned} \boldsymbol{U}=[&l_1^c(\omega, k, z)\boldsymbol{T}_{km}^c(r, \theta)+l_1^s(\omega, k, z)\boldsymbol{T}_{km}^s(r, \theta)\\ &+r_1^c(\omega, k, z)\boldsymbol{S}_{km}^c(r, \theta)+r_1^s(\omega, k, z)\boldsymbol{S}_{km}^s(r, \theta)\\ &+r_2^c(\omega, k, z)\boldsymbol{R}_{km}^c(r, \theta)+r_2^s(\omega, k, z)\boldsymbol{R}_{km}^s(r, \theta)]\exp(-i\omega t),\\ \boldsymbol{T}=[&l_2^c(\omega, k, z)\boldsymbol{T}_{km}^c(r, \theta)+l_2^s(\omega, k, z)\boldsymbol{T}_{km}^s(r, \theta)\\ &+r_3^c(\omega, k, z)\boldsymbol{S}_{km}^c(r, \theta)+r_3^s(\omega, k, z)\boldsymbol{S}_{km}^s(r, \theta)\\ &+r_4^c(\omega, k, z)\boldsymbol{R}_{km}^c(r, \theta)+r_4^s(\omega, k, z)\boldsymbol{R}_{km}^s(r, \theta)]\exp(-i\omega t). \end{aligned} \tag{4}$$

The r, θ dependence of $\boldsymbol{U}$ and $\boldsymbol{T}$ is described by two sets of three orthogonal vector functions defined by

$$\begin{aligned} &\boldsymbol{T}_{km}^c=\frac{1}{kr}\frac{\partial Y_{km}^c}{\partial\theta}\hat{\boldsymbol{r}}-\frac{1}{k}\frac{\partial Y_{km}^c}{\partial r}\hat{\boldsymbol{\theta}},\ \boldsymbol{S}_{km}^c=\frac{1}{k}\frac{\partial Y_{km}^c}{\partial r}\hat{\boldsymbol{r}}+\frac{1}{kr}\frac{\partial Y_{km}^c}{\partial\theta}\hat{\boldsymbol{\theta}},\\ &\boldsymbol{R}_{km}^c=-Y_{km}^c(r, \theta)\hat{\boldsymbol{z}},\ Y_{km}^c(r, \theta)=J_m(kr)\cos m\theta,\\ &\boldsymbol{T}_{km}^s=\frac{1}{kr}\frac{\partial Y_{km}^s}{\partial\theta}\hat{\boldsymbol{r}}-\frac{1}{k}\frac{\partial Y_{km}^s}{\partial r}\hat{\boldsymbol{\theta}},\ \boldsymbol{S}_{km}^s=\frac{1}{k}\frac{\partial Y_{km}^s}{\partial r}\hat{\boldsymbol{r}}+\frac{1}{kr}\frac{\partial Y_{km}^s}{\partial\theta}\hat{\boldsymbol{\theta}},\\ &\boldsymbol{R}_{km}^s=-Y_{km}^s(r, \theta)\hat{\boldsymbol{z}},\ Y_{km}^s(r, \theta)=J_m(kr)\sin m\theta, \end{aligned} \tag{5}$$

where $\hat{\boldsymbol{r}}$, $\hat{\boldsymbol{\theta}}$, and $\hat{\boldsymbol{z}}$ are unit vectors in directions r, θ, z.

The z-dependence is described by two sets of six scalar functions (l_1^c, l_2^c, r_1^c, r_2^c, r_3^c, r_4^c) and (l_1^s, l_2^s, r_1^s, r_2^s, r_3^s, r_4^s). l_i^c and $l_i^s (i=1, 2)$ are made up from the potential χ alone, and separate from the rest to give the SH-wave part of the seismic wavefield and the associated stress. r_i^c and r_i^s $(i=1, 2, 3, 4)$ are made up from the potentials ϕ and ψ, and give the displacements and stresses accompanied by the P- and SV-waves. It can be shown that, as a result of the equation of motion and stress-strain relations of perfect elasticity, the motion-stress vectors $\boldsymbol{f}_l^c(k, m, z, \omega)=(l_1^c, l_2^c)^T$, $\boldsymbol{f}_r^c(k, m, z, \omega)=(r_1^c, r_2^c, r_3^c, r_4^c)^T$, $\boldsymbol{f}_l^s(k, m, z, \omega)=(l_1^s, l_2^s)^T$ and $\boldsymbol{f}_r^s(k, m, z, \omega)=(r_1^s, r_2^s, r_3^s, r_4^s)^T$, where T denotes a transpose, satisfy first-order differential equations of the form

$$\frac{\partial \boldsymbol{f}}{\partial z}=\boldsymbol{A}\boldsymbol{f}. \tag{6}$$

For P-SV waves we have

$$\boldsymbol{A}=\begin{pmatrix} 0 & k & \mu^{-1} & 0\\ -k\lambda[\lambda+2\mu]^{-1} & 0 & 0 & [\lambda+2\mu]^{-1}\\ k^2\zeta-\omega^2\rho & 0 & 0 & k\lambda[\lambda+2\mu]^{-1}\\ 0 & -\omega^2\rho & -k & 0 \end{pmatrix}, \tag{7}$$

where λ and μ are Lamé's constants, ρ is the density, and $\zeta=4\mu[\lambda+\mu]/[\lambda+2\mu]$, and for SH-waves

$$A=\begin{pmatrix} 0 & \mu^{-1} \\ k^2\mu-\omega^2\rho & 0 \end{pmatrix}. \tag{8}$$

The general solution $\boldsymbol{f}$ to the equation $\partial\boldsymbol{f}/\partial z=\boldsymbol{A}\boldsymbol{f}$ is given by

$$\boldsymbol{f}=\boldsymbol{F}\boldsymbol{w}, \tag{9}$$

where $\boldsymbol{F}$ is made up from eigenvectors of $\boldsymbol{A}$ and the associated eigenvalues, and $\boldsymbol{w}$ is a vector of constants weighting the columms of $\boldsymbol{F}$. $\boldsymbol{F}$ is known as the layer matrix and $\boldsymbol{w}$ is the wave vector. For P-SV waves, omitting the superscripts c and s,

$$\begin{pmatrix} r_1 \\ r_2 \\ r_3 \\ r_4 \end{pmatrix}=\boldsymbol{F}\begin{pmatrix} P_D \\ S_D \\ P_U \\ S_U \end{pmatrix}, \tag{10}$$

$$\boldsymbol{F}=\boldsymbol{E}\boldsymbol{\Lambda}=\omega^{-1}\begin{pmatrix} \alpha k & \beta\nu & \alpha k & \beta\nu \\ \alpha\gamma & \beta k & -\alpha\gamma & -\beta k \\ -2\alpha\mu k\gamma & -\beta\mu(k^2+\nu^2) & 2\alpha\mu k\gamma & \beta\mu(k^2+\nu^2) \\ -\alpha\mu(k^2+\nu^2) & -2\beta\mu k\nu & -\alpha\mu(k^2+\nu^2) & -2\beta\mu k\nu \end{pmatrix}$$
$$\times\begin{pmatrix} e^{-\gamma(z-z_{ref})} & 0 & 0 & 0 \\ 0 & e^{-\nu(z-z_{ref})} & 0 & 0 \\ 0 & 0 & e^{\gamma(z-z_{ref})} & 0 \\ 0 & 0 & 0 & e^{\nu(z-z_{ref})} \end{pmatrix}, \tag{11}$$

where P_D and P_U are constants giving the displacement amplitude of downgoing and upgoing P-waves; S_D and S_U are those of downgoing and upgoing SV-waves; and z_{ref} is a reference level for the phase. In a similar way for SH-waves

$$\begin{pmatrix} l_1 \\ l_2 \end{pmatrix}=\boldsymbol{F}\begin{pmatrix} SH_D \\ SH_U \end{pmatrix}, \tag{12}$$

$$\boldsymbol{F}=\boldsymbol{E}\boldsymbol{\Lambda}=\begin{pmatrix} 1 & 1 \\ -\mu\nu & \mu\nu \end{pmatrix}\begin{pmatrix} e^{-\nu(z-z_{ref})} & 0 \\ 0 & e^{\nu(z-z_{ref})} \end{pmatrix}, \tag{13}$$

where SH_D and SH_U are constants giving the displacement amplitude of downgoing and upgoing SH-waves. The inverse of $\boldsymbol{F}$ is given by, for P-SV waves,

$$
\boldsymbol{F}^{-1}=\begin{pmatrix} e^{\gamma(z-z_{ref})} & 0 & 0 & 0 \\ 0 & e^{\nu(z-z_{ref})} & 0 & 0 \\ 0 & 0 & e^{-\gamma(z-z_{ref})} & 0 \\ 0 & 0 & 0 & e^{-\nu(z-z_{ref})} \end{pmatrix} \times \frac{\beta}{2\alpha\mu\gamma\nu\omega}
$$

$$
\times \begin{pmatrix} 2\beta\mu k\gamma\nu & -\beta\mu\nu(k^2+\nu^2) & -\beta k\nu & \beta\gamma\nu \\ -\alpha\mu\gamma(k^2+\nu^2) & 2\alpha\mu k\gamma\nu & \alpha\gamma\nu & -\alpha k\gamma \\ 2\beta\mu k\gamma\nu & \beta\mu\nu(k^2+\nu^2) & \beta k\nu & \beta\gamma\nu \\ -\alpha\mu\gamma(k^2+\nu^2) & -2\alpha\mu k\gamma\nu & -\alpha\gamma\nu & -\alpha k\gamma \end{pmatrix} \tag{14}
$$

and for SH-waves

$$
\boldsymbol{F}^{-1}=\begin{pmatrix} e^{\nu(z-z_{ref})} & 0 \\ 0 & e^{-\nu(z-z_{ref})} \end{pmatrix} \times \frac{1}{2\mu\nu}\begin{pmatrix} \mu\nu & -1 \\ \mu\nu & 1 \end{pmatrix}. \tag{15}
$$

In terms of the propagator matrix $\boldsymbol{P}(z, z_0)$ (Gilbert and Backus, 1966) the solution of $\partial \boldsymbol{f}/\partial z = \boldsymbol{A}\boldsymbol{f}$ with the motion-stress vector specified at some level z_0, $\boldsymbol{f}(z_0)$ is

$$
\boldsymbol{f}(z)=\boldsymbol{P}(z, z_0)\, \boldsymbol{f}(z_0). \tag{16}
$$

Thus $\boldsymbol{P}(z, z_0)$ generates the motion-stress vector at z by operating on the vector at z_0. The propagator matrix has the following properties:

$$
\begin{aligned}
&\boldsymbol{P}(z_0, z_0)=\boldsymbol{I}, \\
&\boldsymbol{P}(z_2, z_1)=\boldsymbol{P}(z_1, z_2)^{-1}, \\
&\boldsymbol{P}(z_2, z_0)=\boldsymbol{P}(z_2, z_1)\, \boldsymbol{P}(z_1, z_0),
\end{aligned} \tag{17}
$$

where $\boldsymbol{I}$ is the unit matrix. For homogeneous layers we may construct the propagator matrix in terms of $\boldsymbol{F}$ in (9) as

$$
\boldsymbol{P}(z, z_0)=\boldsymbol{F}(z)\quad \boldsymbol{F}^{-1}(z_0). \tag{18}
$$

The response of a stratified half-space due to excitation by a source can be obtained by imposing the boundary conditions on the seismic wavefield: the vanishing of the stress at a free surface; a radiation condition in a half-space that the wavefield should consist of either downward propagating waves or evanescent waves decaying with depth; and the action of source in terms of a discontinuity in the motion-stress vector at the source level (e.g., Harkrider, 1964). A formal solution for the displacement field can be found by starting with the radiation conditions and then projecting the motion and stress to the surface using the propagator matrix given by (16). The jumps in motion and stress across the source plane are also projected to the surface and then the displacement field is constructed so that there is no net surface traction. Once solutions for the motion-stress vectors are known, the displacements can be obtained by a superposition of the basic solutions (4) (the inverse Fourier-Hankel transformations)

$$
\begin{aligned}
U_z(r,\theta,z;t)&=\frac{1}{2\pi}\int_{-\infty}^{\infty}\exp(-i\omega t)d\omega\\
&\quad\times\sum_{m=-\infty}^{\infty}\int_0^{\infty}\Big[-r_2^c\cos m\theta-r_2^s\sin m\theta\Big]J_m(kr)kdk,\\
U_r(r,\theta,z;t)&=\frac{1}{2\pi}\int_{-\infty}^{\infty}\exp(-i\omega t)d\omega\\
&\quad\times\sum_{m=-\infty}^{\infty}\int_0^{\infty}\Big[\frac{m}{kr}(-l_1^c\sin m\theta+l_1^s\cos m\theta)J_m(kr)\\
&\quad+(r_1^c\cos m\theta+r_1^s\sin m\theta)J'_m(kr)\Big]kdk,\\
U_\theta(r,\theta,z;t)&=\frac{1}{2\pi}\int_{-\infty}^{\infty}\exp(-i\omega t)d\omega\\
&\quad\times\sum_{m=-\infty}^{\infty}\int_0^{\infty}\Big[-(l_1^c\cos m\theta+l_1^s\sin m\theta)J'_m(kr)\\
&\quad+\frac{m}{kr}(-r_1^c\sin m\theta+r_1^s\cos m\theta)J_m(kr)\Big]kdk,
\end{aligned}
\tag{19}
$$

where $J'_m(kr)=\partial J_m(kr)/\partial(kr)$.

The solutions for the motion-stress vectors using the propagator matrix allow a complete specification of the seismic wavefield but suffer from some computational disadvantages due to growing exponential terms particularly when the frequency is high, as pointed out by Dunkin (1965). In order to avoid the numerical difficulties, Kennett and Kerry (1979) have presented an alternative approach based on the wave-propagator as shown in the next section. We shall follow their approach in deriving the solutions for the motion-stress vectors.

3. The response of a stratified half-space

First we define the reflection and transmission matrices of a portion (z_A, z_C) of a stratified medium by embedding this region between two uniform half spaces in $z<z_A$, $z>z_C$ (Fig. 2). From (16) the motion-stress vectors at the top and bottom of the region are related by

$$\boldsymbol{f}(z_A)=\boldsymbol{P}(z_A,z_C)\,\boldsymbol{f}(z_C). \tag{20}$$

When we combine (9) and (20), the wave vectors in the upper and lower uniform half spaces are related by

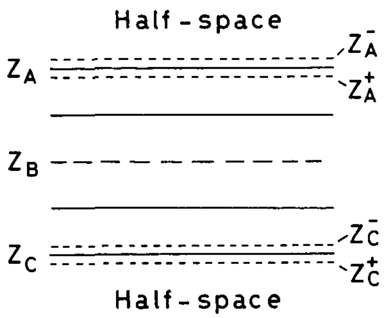

Fig. 2 A stratified medium between two uniform half spaces. $z_A^+(z_C^+)$ is just below the $z_A(z_C)$ interface and $z_A^-(z_C^-)$ is just above the $z_A(z_C)$ interface.

$$\begin{aligned} \boldsymbol{w}(z_A^-) &= \boldsymbol{E}^{-1}(z_A^-)\ \boldsymbol{P}(z_A,\ z_C)\ \boldsymbol{E}(z_C^+)\ \boldsymbol{w}(z_C^+) \\ &= \boldsymbol{Q}(z_A^-,\ z_C^+)\ \boldsymbol{w}(z_C^+), \end{aligned} \tag{21}$$

and by analogy with (16) $\boldsymbol{Q}$ is called as the wave-propagator (Kennett and Kerry, 1979). The wave-propagator has similar properties to the propagator matrix in (17)

$$\begin{aligned} \boldsymbol{Q}(z_A,\ z_C) &= \boldsymbol{Q}(z_A,\ z_B)\ \boldsymbol{Q}(z_B,\ z_C), \\ \boldsymbol{Q}(z_A,\ z_C) &= \boldsymbol{Q}^{-1}(z_C,\ z_A). \end{aligned} \tag{22}$$

Although $\boldsymbol{P}(z_A,\ \xi)$ will be continuous across a plane $z=\xi$, the wave-propagator will not be unless the elastic parameters are continuous across ξ. Thus in (21) the $+$, $-$ indicators are strictly necessary (see Fig. 2).

We split the wave vectors in the uniform half spaces into their up and downgoing wave parts and partition $\boldsymbol{Q}(z_A,\ z_C)$ so that (21) becomes

$$\begin{pmatrix} \boldsymbol{w}_D(z_A^-) \\ \cdots\cdots \\ \boldsymbol{w}_U(z_A^-) \end{pmatrix} = \begin{pmatrix} \boldsymbol{Q}_{DD} & \vdots & \boldsymbol{Q}_{DU} \\ \cdots & \vdots & \cdots \\ \boldsymbol{Q}_{UD} & \vdots & \boldsymbol{Q}_{UU} \end{pmatrix} \begin{pmatrix} \boldsymbol{w}_D(z_C^+) \\ \cdots\cdots \\ \boldsymbol{w}_U(z_C^+) \end{pmatrix}. \tag{23}$$

According to Kennett and Kerry (1979), we may define reflection and transmission matrices $\boldsymbol{R}$, $\boldsymbol{T}$ from (23). For incident downgoing waves from the half-space $z<z_A$, the transmission and reflection matrices are given by

$$\begin{aligned} \boldsymbol{T}_D^{AC} &= (\boldsymbol{Q}_{DD})^{-1}, \\ \boldsymbol{R}_D^{AC} &= \boldsymbol{Q}_{UD}(\boldsymbol{Q}_{DD})^{-1}, \end{aligned} \tag{24}$$

and with incident upgoing waves in $z>z_C$ they are

$$\begin{aligned} \boldsymbol{T}_U^{AC} &= \boldsymbol{Q}_{UU} - \boldsymbol{Q}_{UD}(\boldsymbol{Q}_{DD})^{-1}\ \boldsymbol{Q}_{DU}, \\ \boldsymbol{R}_U^{AC} &= -(\boldsymbol{Q}_{DD})^{-1}\ \boldsymbol{Q}_{DU}. \end{aligned} \tag{25}$$

For P-SV waves reflection and transmission matrices are 2×2 matrices but for SH-waves they are just the coefficients. The wave-propagator takes the form

$$Q(z_A^-,\ z_C^+)=\left(\begin{array}{c:c} (T_D^{AC})^{-1} & -(T_D^{AC})^{-1}\ R_U^{AC} \\ \hdashline R_D^{AC}(T_D^{AC})^{-1} & T_U^{AC}-R_D^{AC}(T_D^{AC})^{-1}\ R_U^{AC} \end{array}\right). \tag{26}$$

When the region $(z_A,\ z_C)$ is divided by splitting the stratification at a level z_B between z_A and z_C (Fig. 2), the reflection and transmission matrices for the entire region can be given by those for the upper region 'AB' and the lower region 'BC'. Combining the first equation in (22) and (26), the overall reflection and transmission matrices are

$$\begin{aligned} T_D^{AC}&=T_D^{BC}[I-R_U^{AB}\ R_D^{BC}]^{-1}\ T_D^{AB},\\ R_D^{AC}&=R_D^{AB}+T_U^{AB}\ R_D^{BC}[I-R_U^{AB}\ R_D^{BC}]^{-1}\ T_D^{AB},\\ T_U^{AC}&=T_U^{AB}[I-R_D^{BC}\ R_U^{AB}]^{-1}\ T_U^{BC},\\ R_U^{AC}&=R_U^{BC}+T_D^{BC}\ R_U^{AB}[I-R_D^{BC}\ R_U^{AB}]^{-1}\ T_U^{BC}. \end{aligned} \tag{27}$$

These are addition rules for the reflection and transmission matrices. In (27) the matrix inverse $[I-R_U^{AB}\ R_D^{BC}]^{-1}$ corresponds to a reverberation operator for the region 'AC'.

We construct the reflection and transmission matrices for an interface at $z=z_I$. From (21) the wave-propagator for the interface is

$$\begin{aligned} Q(z_I^-,\ z_I^+)&=E^{-1}(z_I^-)\ P(z_I,\ z_I)\ E(z_I^+)\\ &=E^{-1}(z_I^-)\ E(z_I^+) \end{aligned} \tag{28}$$

since $P(z_I,\ z_I)=I$. If we substitute partitioned forms of Q in (28) into (24) and (25), we can construct the reflection and transmission matrices for the interface. For P-SV waves they become considerably complicated forms, but for SH-waves they have simple forms as

$$\begin{aligned} R_{D,SH}^I&=\frac{\nu_1\mu_1-\nu_2\mu_2}{\nu_1\mu_1+\nu_2\mu_2}, & T_{D,SH}^I&=\frac{2\nu_1\mu_1}{\nu_1\mu_1+\nu_2\mu_2},\\ R_{U,SH}^I&=-R_{D,SH}^I, & T_{U,SH}^I&=\frac{2\nu_2\mu_2}{\nu_1\mu_1+\nu_2\mu_2}, \end{aligned} \tag{29}$$

where subscripts 1 and 2 indicate the upper $(z<z_I)$ and lower $(z>z_I)$ regions.

In the special case of a uniform layer $(z_A\le z\le z_C)$, the wave-propagator is given by

$$Q(z_A,\ z_C)=\Lambda(z_A)\ \Lambda^{-1}(z_C). \tag{30}$$

For P-SV waves

$$Q(z_A, z_C)=\left(\begin{array}{cc:cc} e^{-\gamma(z_A-z_C)} & 0 & 0 & 0 \\ 0 & e^{-\nu(z_A-z_C)} & 0 & 0 \\ \hdashline 0 & 0 & e^{\gamma(z_A-z_C)} & 0 \\ 0 & 0 & 0 & e^{\nu(z_A-z_C)} \end{array}\right)$$

$$=\left(\begin{array}{c:c} \boldsymbol{D}^{-1} & \mathbf{0} \\ \hdashline \mathbf{0} & \boldsymbol{D} \end{array}\right), \tag{31}$$

where $\boldsymbol{D}$ is the phase income matrix for downward propagation from z_A to z_C. Comparing (31) with (26), we have the reflection and transmission matrices for the uniform layer as

$$\begin{aligned} \boldsymbol{T}_D^{AC}&=\boldsymbol{D}, & \boldsymbol{T}_U^{AC}&=\boldsymbol{D}, \\ \boldsymbol{R}_D^{AC}&=\mathbf{0}, & \boldsymbol{R}_U^{AC}&=\mathbf{0}. \end{aligned} \tag{32}$$

For SH-waves

$$\boldsymbol{Q}(z_A, z_C)=\begin{pmatrix} e^{-\nu(z_A-z_C)} & 0 \\ 0 & e^{\nu(z_A-z_C)} \end{pmatrix}=\begin{pmatrix} D^{-1} & 0 \\ 0 & D \end{pmatrix}, \tag{33}$$

and

$$\begin{aligned} T_{D,SH}^{AC}&=D, & T_{U,SH}^{AC}&=D, \\ R_{D,SH}^{AC}&=0, & R_{U,SH}^{AC}&=0. \end{aligned} \tag{34}$$

In the uniform layer the reflection matrices vanish and transmission through the layer gives phase terms, as would be expected.

For a stack of uniform layers the reflection and transmission matrices may be constructed by the phase delays through a layer and the interface coefficients in terms of the addition rules (27). Consider a uniform layer in $z_1<z<z_2$ overlying a pile of such layers in $z_2<z<z_3$. We suppose the reflection and transmission matrices at z_2^- just into the layer are known and write e.g. $\boldsymbol{R}_D(z_2^-)=\boldsymbol{R}_D(z_2^-, z_3^+)$. We may add in the phase terms corresponding to transmission through the uniform layer using the addition rules (27) and (32). Then the reflection and transmission matrices just below the interface at z_1^+ are given by

$$\begin{aligned} \boldsymbol{T}_D(z_1^+)&=\boldsymbol{T}_D(z_2^-)\ \boldsymbol{D}^{12}, \\ \boldsymbol{R}_D(z_1^+)&=\boldsymbol{D}^{12}\ \boldsymbol{R}_D(z_2^-)\ \boldsymbol{D}^{12}, \\ \boldsymbol{T}_U(z_1^+)&=\boldsymbol{D}^{12}\ \boldsymbol{T}_U(z_2^-), \end{aligned} \tag{35}$$

where $\boldsymbol{D}^{12}$ is the phase income for downward propagation through the layer (see (31)). A further application of the addition rules allows us to include the reflection and transmission matrices for the interface z_1, e.g. $\boldsymbol{R}_D^1=\boldsymbol{R}_D(z_1^-, z_1^+)$. The reflection and transmission matrices just above the z_1 interface are given by

$$
\begin{aligned}
\boldsymbol{T}_D(z_1^-) &= \boldsymbol{T}_D(z_1^+)\,[\boldsymbol{I}-\boldsymbol{R}_U^1\,\boldsymbol{R}_D(z_1^+)\,]^{-1}\,\boldsymbol{T}_D^1, \\
\boldsymbol{R}_D(z_1^-) &= \boldsymbol{R}_D^1+\boldsymbol{T}_U^1\,\boldsymbol{R}_D(z_1^+)[\boldsymbol{I}-\boldsymbol{R}_U^1\,\boldsymbol{R}_D(z_1^+)\,]^{-1}\,\boldsymbol{T}_D^1, \\
\boldsymbol{T}_U(z_1^-) &= \boldsymbol{T}_U^1[\boldsymbol{I}-\boldsymbol{R}_D(z_1^+)\,\boldsymbol{R}_U^1]^{-1}\,\boldsymbol{T}_U(z_1^+), \\
\boldsymbol{R}_U(z_1^-) &= \boldsymbol{R}_U(z_2^-)+\boldsymbol{T}_D(z_1^+)\,\boldsymbol{R}_U^1[\boldsymbol{I}-\boldsymbol{R}_D(z_1^+)\,\boldsymbol{R}_U^1]^{-1}\,\boldsymbol{T}_U(z_1^+).
\end{aligned}
\tag{36}
$$

These two applications of the addition rules may be used recursively to calculate the overall reflection and transmission matrices, by starting at the base of the layers. The recursive scheme is numerically stable even at high frequencies because no exponential terms which grow with frequency will appear in $\boldsymbol{D}^{12}$.

When a vertical inhomogeneous region is bounded above by the free surface, we may introduce the free surface reflection matrix $\tilde{\boldsymbol{R}}$. We partition $\boldsymbol{E}$ matrix in (11) as

$$
\boldsymbol{E}=\begin{pmatrix} \boldsymbol{M}_D & \vdots & \boldsymbol{M}_U \\ \cdots & \cdot & \cdots \\ \boldsymbol{N}_D & \vdots & \boldsymbol{N}_U \end{pmatrix}
\tag{37}
$$

so that $\boldsymbol{M}_D$, $\boldsymbol{M}_U$ are the displacement transformations and $\boldsymbol{N}_D$, $\boldsymbol{N}_U$ the stress transformations. For the P-SV wave system $\boldsymbol{M}_D$ etc. will be 2×2 matrices and for SH-waves simply scalars. In terms of the partitions of $\boldsymbol{E}$ the free surface boundary condition of vanishing traction at $z=0$ is, from (9),

$$
\begin{pmatrix} \boldsymbol{r}_0 \\ \cdots \\ \boldsymbol{0} \end{pmatrix}=\begin{pmatrix} \boldsymbol{M}_D & \vdots & \boldsymbol{M}_U \\ \cdots & \cdot & \cdots \\ \boldsymbol{N}_D & \vdots & \boldsymbol{N}_U \end{pmatrix}\begin{pmatrix} \boldsymbol{w}_D(z_0^+) \\ \cdots \\ \boldsymbol{w}_U(z_0^+) \end{pmatrix},
\tag{38}
$$

where $\boldsymbol{r}_0$ is the surface displacement field. Thus the free surface reflection matrix is

$$
\tilde{\boldsymbol{R}}=-\boldsymbol{N}_D^{-1}\,\boldsymbol{N}_U.
\tag{39}
$$

For P-SV waves, from (11) and (37),

$$
\tilde{\boldsymbol{R}}=\frac{1}{(k^2+\nu^2)^2-4\nu\gamma k^2}\begin{pmatrix} -[\,(k^2+\nu^2)^2+4\nu\gamma k^2] & -4\beta k\nu(k^2+\nu^2)/\alpha \\ 4\alpha k\gamma(k^2+\nu^2)/\beta & [\,(k^2+\nu^2)^2+4\nu\gamma k^2] \end{pmatrix}
\tag{40}
$$

and for SH-waves, from (13),

$$
\tilde{\boldsymbol{R}}_{SH}=1.
\tag{41}
$$

At the free surface the displacement matrix due to an incident upgoing wave is, from (38),

$$
\boldsymbol{r}_0=(\boldsymbol{M}_U+\boldsymbol{M}_D\tilde{\boldsymbol{R}})\;\boldsymbol{w}_U,
\tag{42}
$$

where $(\boldsymbol{M}_U+\boldsymbol{M}_D\tilde{\boldsymbol{R}})$ is called as the receiver function matrix. For P-SV waves

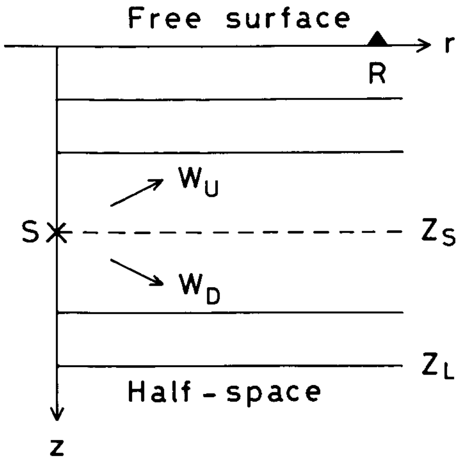

Fig. 3 Configuration of elastic half-space with a source (S) at depth z_S and a receiver (R) at a free surface. Beneath z_L the medium has uniform properties so that a radiation condition has to be applied at this level. The conventions for up and downgoing waves are also indicated.

$$(\boldsymbol{M}_U+\boldsymbol{M}_D\tilde{\boldsymbol{R}})=\omega^{-1}\begin{pmatrix}-4\alpha\nu\gamma k(k^2-\nu^2)/C & -2\beta\nu(k^2+\nu^2)\ (k^2-\nu^2)/C \\ 2\alpha\gamma(k^2+\nu^2)\ (k^2-\nu^2)/C & 4\beta\nu\gamma k(k^2-\nu^2)/C\end{pmatrix}, \tag{43}$$

where $C=(k^2+\nu^2)^2-4\nu\gamma k^2$, and for SH-waves

$$(\boldsymbol{M}_{U,SH}+\boldsymbol{M}_{D,SH}\ \tilde{\boldsymbol{R}}_{SH})=2. \tag{44}$$

Using the reflection and transmission properties of elastic media mentioned above, we can generate the displacement field in a stratified half-space due to excitation of a source. We consider the half space illustrated in Fig. 3 with a source at the level z_S and a uniform half space beneath z_L. The boundary conditions are the vanishing of the stress at the free surface, the radiation condition in the half-space, and the discontinuity in the motion-stress vector at the source level as the action of source. For a point source there will be a jump in the motion-stress vector across the source plane

$$\boldsymbol{f}(k,\ m,\ z_S^+,\ \omega)-\boldsymbol{f}(k,\ m,\ z_S^-,\ \omega)=\boldsymbol{S}(k,\ m,\ z_S,\ \omega). \tag{45}$$

An alternative approach to the introduction of a source is to regard it as giving rise to a discontinuity in the wave vector (Haskell, 1964 ; Harkrider, 1964)

$$\begin{aligned}\boldsymbol{w}(k,\ m,\ z_S^+,\ \omega)-\boldsymbol{w}(k,\ m,\ z_S^-,\ \omega)&=\boldsymbol{\Sigma}(k,\ m,\ z_S,\ \omega)\\ &=\boldsymbol{F}^{-1}(k,\ z_S)\ \boldsymbol{S}(k,\ m,\ z_S,\ \omega).\end{aligned} \tag{46}$$

In the jump vector $\boldsymbol{\Sigma}=(\boldsymbol{\Sigma}_D,\ -\boldsymbol{\Sigma}_U)^T$, a source will radiate $\boldsymbol{\Sigma}_D$ downwards and $\boldsymbol{\Sigma}_U$ upwards.

According to Kennett and Kerry (1979) the surface response due to a buried source takes the form

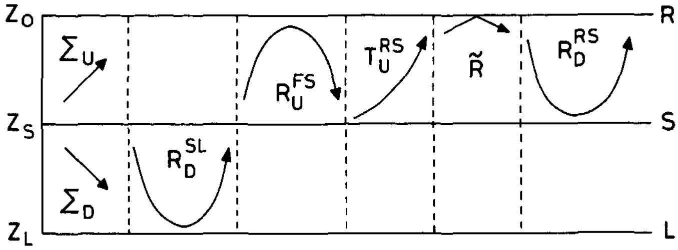

Fig. 4 Schematic diagram of the major elements in the surface response from a source at depth z_S(equation (47)).

$$\boldsymbol{r}_0=(\boldsymbol{M}_U+\boldsymbol{M}_D\tilde{\boldsymbol{R}})[\boldsymbol{I}-\boldsymbol{R}_D^{RS}\tilde{\boldsymbol{R}}]^{-1}\ \boldsymbol{T}_U^{RS}[\boldsymbol{I}-\boldsymbol{R}_D^{SL}\ \boldsymbol{R}_U^{FS}]^{-1}(\boldsymbol{R}_D^{SL}\ \boldsymbol{\Sigma}_D+\boldsymbol{\Sigma}_U). \quad (47)$$

A schematic diagram of the major elements in (47) is given in Fig. 4. The expression $(\boldsymbol{M}_U+\boldsymbol{M}_D\tilde{\boldsymbol{R}})$ is the operator which converts an upgoing wave into a free surface displacement (see (42)). The source contribution $(\boldsymbol{R}_D^{SL}\ \boldsymbol{\Sigma}_D+\boldsymbol{\Sigma}_U)$ corresponds to the entire upward radiation associated with the source at the level $z=z_S$. The term $[\boldsymbol{I}-\boldsymbol{R}_D^{SL}\ \boldsymbol{R}_U^{FS}]^{-1}$ corresponds to a reverberation operator through the whole half space, coupling the upper and lower parts at the level $z=z_S$. The composite action $[\boldsymbol{I}-\boldsymbol{R}_D^{SL}\ \boldsymbol{R}_U^{FS}]^{-1}\ (\boldsymbol{R}_D^{SL}\ \boldsymbol{\Sigma}_D+\boldsymbol{\Sigma}_U)$ is thus to produce, at the level $z=z_S$, a sequence of wave groups corresponding to radiation from the source. Each of these wave groups is then projected to the surface by the transmission term $\boldsymbol{T}_U^{RS}$. The reverberation operator $[\boldsymbol{I}-\boldsymbol{R}_D^{RS}\ \tilde{\boldsymbol{R}}]^{-1}$ corresponds to channelling between the source and the surface. Each of the infinite sequence of wave groups at the source level z_S will thus suffer a further infinite surface interaction, to produce the entire displacement response at the surface.

4. Shear dislocation and explosive sources

Here we derive the jump in the wave vector across the source plane for a point shear dislocation source. We consider the dislocation source located at depth $z=h$ (Fig. 5) with the moment function $M(t)$. According to Harkrider (1976) and Sato (1969), the scalar potentials for the dislocation source corresponding to (1) and (3) are given by, in the frequency domain,

$$\begin{aligned}
\phi(r,\ \theta,\ z\ ;\ \omega)&=\frac{M(\omega)}{4\pi\rho\omega^2}\sum_{m=0}^{2}\Lambda_m\int_0^\infty A_mF_\alpha J_m(kr)dk,\\
\psi(r,\ \theta,\ z\ ;\ \omega)&=\frac{M(\omega)}{4\pi\rho\omega^2}\sum_{m=0}^{2}\Lambda_m\int_0^\infty B_mF_\beta J_m(kr)dk, \qquad (48)\\
\chi(r,\ \theta,\ z\ ;\ \omega)&=\frac{M(\omega)}{4\pi\rho\omega^2}\sum_{m=0}^{2}\Lambda_{m+3}\int_0^\infty C_mF_\beta J_m(kr)dk,
\end{aligned}$$

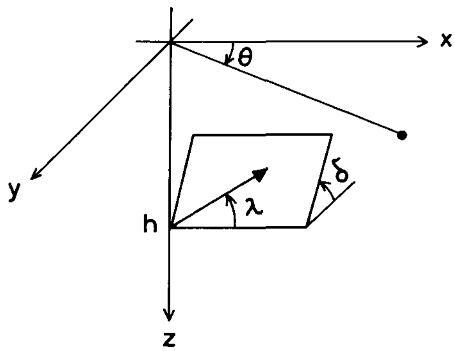

Fig. 5 Coordinate system of the shear dislocation source. λ=rake angle, δ=dip angle, and θ=azimuth from the fault strike.

where

$$
\begin{aligned}
&\Lambda_0=\frac{1}{2}\sin\lambda\sin 2\delta,\\
&\Lambda_1=\cos\lambda\cos\delta\cos\theta-\sin\lambda\cos 2\delta\sin\theta,\\
&\Lambda_2=\frac{1}{2}\sin\lambda\sin 2\delta\cos 2\theta+\cos\lambda\sin\delta\sin 2\theta,\\
&\Lambda_3=0,\\
&\Lambda_4=-\cos\lambda\cos\delta\sin\theta-\sin\lambda\cos 2\delta\cos\theta,\\
&\Lambda_5=-\frac{1}{2}\sin\lambda\sin 2\delta\sin 2\theta+\cos\lambda\sin\delta\cos 2\theta,\\
&\lambda=\text{rake angle},\quad \delta=\text{dip angle},\\
&\theta=\text{azimuth from the fault strike},\\
&M(\omega)=\text{spectrum moment},\\
&A_0=k^2+2\gamma^2,\quad A_1=-2\epsilon k\gamma,\quad A_2=k^2,\\
&B_0=3\epsilon\nu,\quad B_1=(k_\beta^2-2k^2)/k,\quad B_2=\epsilon\nu,\\
&C_0=0,\quad C_1=\epsilon k_\beta^2\nu/k,\quad C_2=-k_\beta^2,\\
&k_\alpha=\omega/\alpha,\quad k_\beta=\omega/\beta,\quad \epsilon=\mathrm{sgn}(z-h),
\end{aligned}
\tag{49}
$$

and

$$F_\alpha=\frac{k\exp(-\gamma\,|\,z-h\,|\,)}{\gamma},\quad F_\beta=\frac{k\exp(-\nu\,|\,z-h\,|\,)}{\nu}.$$

If we substitute these potentials into (1), we find the discontinuity in the motion-stress vector (45) for the dislocation source. Then we obtain the jump in the wave vector from (46). After all, for a buried dislocation source in the stratified media the free surface displacements are, in the time domain,

$$U_z(r,\theta,z\,;\,t)=\frac{1}{2\pi}\int_{-\infty}^{\infty}\exp(-i\omega t)d\omega\,\frac{M(\omega)}{4\pi\rho\omega^2}\sum_{m=0}^{2}\Lambda_m(\lambda,\delta,\theta)$$

$$\times \int_0^\infty [-r_2^m]\ J_m(kr)kdk,$$

$$\begin{aligned} U_r(r,\ \theta,\ z\ ;\ t) &= \frac{1}{2\pi}\int_{-\infty}^{\infty} \exp(-i\omega t)dw\ \frac{M(\omega)}{4\pi\rho\omega^2}\sum_{m=0}^{2}\Lambda_m(\lambda,\ \delta,\ \theta) \\ &\times \int_0^\infty [r_1^m J_m'(kr) - l_1^m\ \frac{m}{kr}\ J_m(kr)]kdk, \\ U_\theta(r,\ \theta,\ z\ ;\ t) &= \frac{1}{2\pi}\int_{-\infty}^{\infty} \exp(-i\omega t)d\omega\ \frac{M(\omega)}{4\pi\rho\omega^2}\sum_{m=0}^{2}\Lambda_{m+3}(\lambda,\ \delta,\ \theta) \\ &\times \int_0^\infty [r_1^m \frac{m}{kr}\ J_m(kr) - l_1^m\ J_m'(kr)]kdk, \end{aligned} \tag{50}$$

where r_1^m, r_2^m and l_1^m are given by, from (47),

$$\begin{aligned} \begin{pmatrix} r_1^m \\ r_2^m \end{pmatrix} &= (\boldsymbol{M}_U + \boldsymbol{M}_D\tilde{\boldsymbol{R}})\ [\boldsymbol{I} - \boldsymbol{R}_D^{RS}\tilde{\boldsymbol{R}}]^{-1}\ \boldsymbol{T}_U^{RS}[\boldsymbol{I} - \boldsymbol{R}_D^{SL}\ \boldsymbol{R}_U^{FS}]^{-1} \\ &\times \left[\ \boldsymbol{R}_D^{SL}\begin{pmatrix} P_D^m \\ SV_D^m \end{pmatrix} + \begin{pmatrix} P_U^m \\ SV_U^m \end{pmatrix}\right], \\ l_1^m &= 2[1 - R_{D,SH}^{RS}]^{-1}\ T_{U,SH}^{RS}[1 - R_{D,SH}^{SL}\ R_{U,SH}^{FS}]^{-1} \\ &\times [R_{D,SH}^{SL}\ SH_D^m + SH_U^m], \end{aligned} \tag{51}$$

with

$$\begin{aligned} &P^0 = \frac{\omega}{\alpha\gamma}(3k^2 - 2k_\alpha^2), && SV^0 = -\frac{3\omega k}{\beta}, && SH^0 = 0, \\ &P^1 = -\epsilon\frac{2\omega k}{\alpha}, && SV^1 = \epsilon\frac{\omega(2k^2 - k_\beta^2)}{\beta\nu}, && SH^1 = \epsilon k_\beta^2, \\ &P^2 = \frac{\omega k^2}{\alpha\gamma}, && SV^2 = -\frac{\omega k}{\beta}, && SH^2 = -\frac{k\ k_\beta^2}{\nu}, \end{aligned} \tag{52}$$

and

$$\epsilon = \begin{cases} -1 & \text{for } U \text{ subscript} \\ 1 & \text{for } D \text{ subscript.} \end{cases}$$

For an explosive type source the scalar potentials are, in the frequency domain,

$$\begin{aligned} &\phi(r,\ \theta,\ z\ ;\ \omega) = \frac{F(\omega)}{4\pi\rho\alpha^2}\int_0^\infty \frac{kJ_0(kr)\exp(-\gamma\,|\,z-h\,|\,)}{\gamma}dk, \\ &\psi(r,\ \theta,\ z\ ;\ \omega) = 0, \\ &\chi(r,\ \theta,\ z\ ;\ \omega) = 0, \end{aligned} \tag{53}$$

and the surface displacements are, in the time domain,

$$U_z(r,\ \theta,\ z\ ;\ t)=\frac{1}{2\pi}\int_{-\infty}^{\infty}\exp(-i\omega t)d\omega\frac{F(\omega)}{4\pi\rho\alpha^2}\int_0^{\infty}[-r_2^0]J_0(kr)kdk,$$
$$U_r(r,\ \theta,\ z\ ;\ t)=\frac{1}{2\pi}\int_{-\infty}^{\infty}\exp(-i\omega t)d\omega\frac{F(\omega)}{4\pi\rho\alpha^2}\int_0^{\infty}r_1^0J'_0(kr)kdk, \tag{54}$$
$$U_\theta(r,\ \theta,\ z\ ;\ t)=0,$$

where $F(\omega)$=Fourier transform of the source time function, and

$$\begin{pmatrix} r_1^0 \\ r_2^0 \end{pmatrix}=(\boldsymbol{M}_U+\boldsymbol{M}_D\tilde{\boldsymbol{R}})\ [\boldsymbol{I}-\boldsymbol{R}_D^{RS}\tilde{\boldsymbol{R}}]^{-1}\ \boldsymbol{T}_U^{RS}[\boldsymbol{I}-\boldsymbol{R}_D^{SL}\ \boldsymbol{R}_U^{FS}]^{-1}$$
$$\times\left[\ \boldsymbol{R}_D^{SL}\begin{pmatrix} P^0 \\ 0 \end{pmatrix}+\begin{pmatrix} P^0 \\ 0 \end{pmatrix}\right] \tag{55}$$

with
$$P^0=\frac{\omega}{\alpha\gamma}.$$

The source potentials of the form (1) for various force systems have been given by Onda et al. (1975).

5. Computational aspects

First we construct $\boldsymbol{R}_D^{SL}$, $\boldsymbol{R}_U^{FS}$, $\boldsymbol{T}_U^{RS}$, $\boldsymbol{R}_D^{RS}$ and $\tilde{\boldsymbol{R}}$ for one frequency ω and many wavenumbers k specified by (58), using the iterative technique for calculating the reflection and transmission matrices. Then we construct the surface displacement scalars r_1^m, r_2^m, l_1^m from (51).

Next we carry out the wavenumber integration which involves quantities of the form

$$I_m=\int_0^{\infty}F(k,\ \omega)\ J_m(kr)\ k\ dk \quad m=0, 1, 2. \tag{56}$$

The kernel $F(k,\ \omega)$ depends upon wavenumber, frequency, source depth, and layer properties. According to Bouchon (1981) the wavenumber integration (56) can be evaluated by a discrete wavenumber summation

$$I_m=\frac{\pi}{L}\sum_{j=0}^{\infty}\epsilon_jk_j\ F(k_j,\ \omega)\ J_m(k_jr), \tag{57}$$

where

$$\epsilon_j=\begin{cases}2 & \text{for } j\neq 0\\ 1 & \text{for } j=0\end{cases}\text{'}$$
$$k_j=2\pi j/L, \tag{58}$$

and L is an equal radial interval for a circular source array. The representation (57) is valid as long as relations $r<L/2$ and $[(L-r)^2+z^2]^{1/2}>\alpha t$ are satisfied. To avoid the influence of the singularities of the integrand $F(k, \omega)$, and the discretization, we give to the frequency an imaginary part, the effect of which is later removed from the time domain solution. This procedure is described in detail by Bouchon (1979). The k loop in (57) is stopped if

$$\frac{|k_j F(k_j, \omega) J_m(k_j r)|}{|\sum_{i=0}^{j} k_i F(k_i, \omega) J_m(k_i r)|} < e, \tag{59}$$

where e is a previously specified precision. The loop will not be terminated by a zero of the Bessel functions.

We can obtain the spectra of the seismograms which would be recorded at an observation point, by performing the above calculations at different frequencies and including the source spectrum. Finally the inversion to the time domain is performed by using the fast Fourier transform.

6. Numerical examples

Our first set of examples illustrates the effect of a single surface layer on seismograms for local earthquakes, comparing with seismograms for a half-space model. Parameters of the single layer model are shown in Fig. 6. For the crust half-space model we take parameters of $\alpha = 6$ km/sec, $\beta = 3.5$ km/sec and $\rho = 2.7$ g/cm^3. We look at the varying response to a dislocation source with $\lambda = 30°$, $\delta = 60°$, $\theta = 30°$ at 20 km depth (Fig. 7). The source time function adopted is

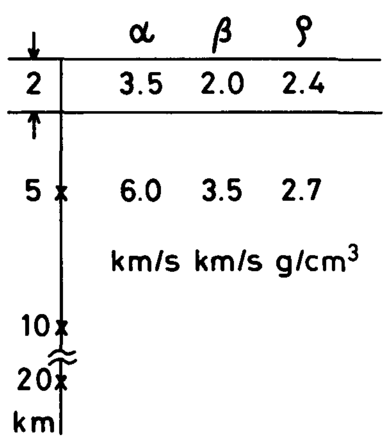

Fig. 6 Layer parameters for the single layer over a half -space model for local earthquake calculations. The three focal depths used are indicated.

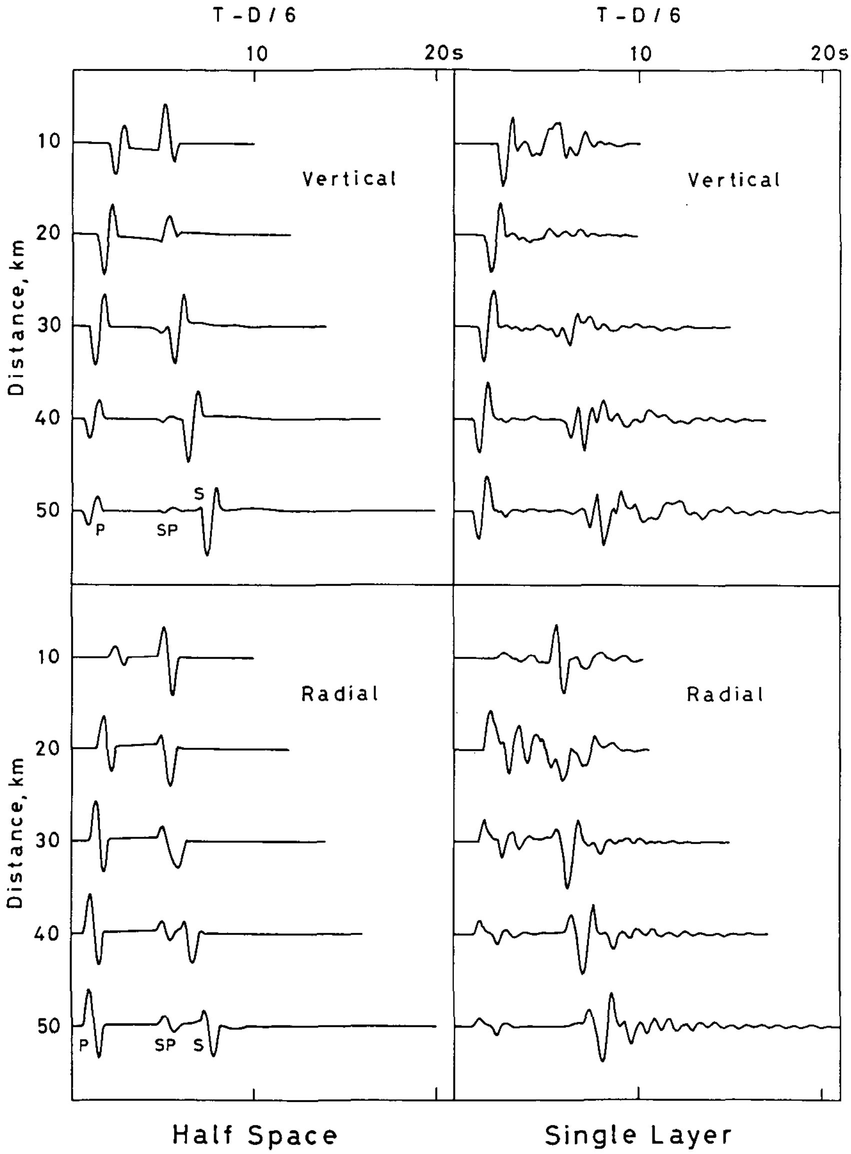

Fig. 7 Synthetic seismograms at various distances for the half-space and the single layer models due to the dislocation source with $\lambda=30^{\circ}$, $\delta=60^{\circ}$ and $\theta=30^{\circ}$. The focal depth is 20 km and the source time function has T_0 of 1 sec. Amplitude is normalized.

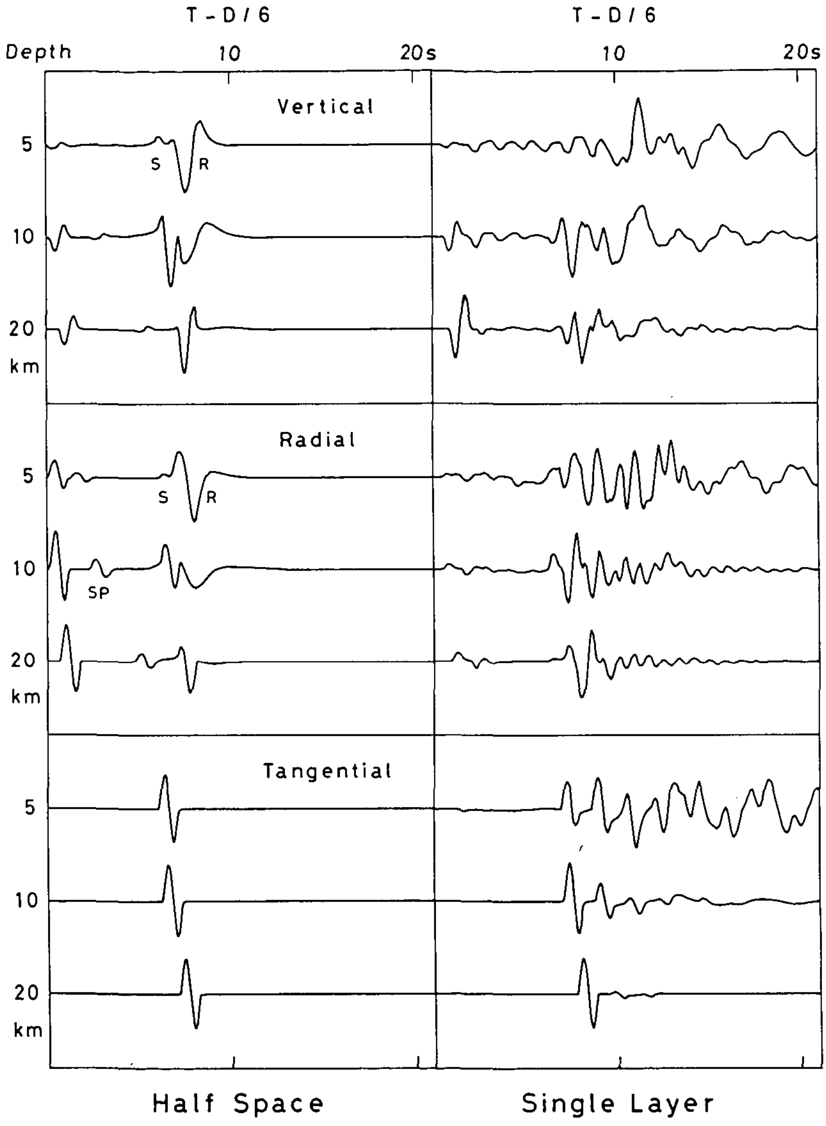

Fig. 8 Synthetic seismograms for various focal depths for the half-space and the single layer models due to the dislocation source with $\lambda=30°$, $\delta=60°$ and $\theta=30°$. The distance is 50 km and the source time function has T_0 of 1 sec. Amplitude is normalized.

$$M(t)=\frac{1}{2}\left[1+\cos\omega_0\left(t-\frac{\pi}{\omega_0}\right)\right] \quad 0\leq t\leq\frac{2\pi}{\omega_0}=T_0$$
$$=0 \quad t<0,\ t>T_0. \tag{60}$$

The far-field displacement for this time function is a one cycle sine wave with a period of $T_0=2\pi/\omega_0$(Sasatani, 1984).

We have no significant surface waves in the seismograms in Fig. 7 because of the deep source. The seismograms for the half-space model are simply made up of P, SP and S phases, but those for the single layer model have complex forms influenced strongly by reverberations in the surface channel.

The second set of examples illustrates the effect of varying the focal depth (5, 10, 20 km depth) with the fixed source mechanism as used above (Fig. 8). The seismograms from the shallowest source (5 km depth) show that as expected the surface waves become predominant phases for both crustal models. For the single layer model, the main phase is preceded by a rather osillatory higher mode train, especially in the radial component. The combinations of P and S reflections in the surface layer lead to a very complex reverberation sequence on vertical and radial components, compared with the purely S reflections on the tangential component. From Figs. 7 and 8 we can see that surface reflected phases play an important role in shaping the nature of the seismograms.

Acknowledgements

The numerical calculations were carried out by HITAC M-280 H at the Hokkaido University Computing Center.

References

Aki, K., and P.G. Richards, 1980. Quantitative seismology. vol. 1, pp. 1-557, W.H. Freeman and Company.

Bouchon, M., 1979. Discrete wave number representation of elastic wave fields in three-space dimensions. J. Geophys. Res., **84**, 3609-3614.

Bouchon, M., 1981. A simple method to calculate Green's functions for elastic layered media. Bull. Seism. Soc. Am., **71**, 959-971.

Dunkin, J.W., 1965. Computation of modal solutions in layered, elastic media at high frequencies. Bull. Seism. Soc. Am., **55**, 335-358.

Fuchs, K. and G. Müller, 1971. Computation of synthetic seismograms with the reflectivity method and comparison with observations. Geophys. J.R. astr. Soc., **23**, 417-433.

Gilbert, F. and G.E. Backus, 1966. Propagator matrices in elastic wave and vibration problems. Geophys., **31**, 326-332.

Harkrider, D.G., 1964. Surface waves in multilayered elastic media : I-Rayleigh and Love waves from buried sources in a multilayered elastic half space. Bull. Seism. Soc.

Am., **54**, 624-679.
Harkrider, D.G., 1976. Potentials and displacements for two theoretical seismic sources. Geophys. J.R. astr. Soc., **47**, 97-133.
Haskell, N.A., 1764. Radiation pattern of surface waves from point sources in a multilayered medium. Bull. Seism. Soc. Am., **54**, 377-393.
Helmberger, D.V., 1968. The crust-mantle transition in the Bering Sea. Bull. Seism. Soc. Am., **58**, 179-214.
Kennett, B.L.N., 1983. Seismic wave propagation in stratified media. Cambridge monograph on mechanics and applied mathematics, pp. 1-342, Cambridge University Press.
Kennett, B.L.N. and N.J. Kerry, 1979. Seismic waves in a stratified half-space. Geophys. J. R. astr. Soc., **57**, 557-583.
Kind, R., 1978. The reflectivity method for a buried source. J. Geophys., **44**, 603-612.
Lamb, H. 1904. On the propagation of tremors at the surface of an elastic solid. Phil. Trans. Roy. Soc. London, Ser. A, **203**, 1-42.
Onda, I., S. Komaki, and M. Ichikawa, 1975. Theoretical and experimental studies of a shear wave generator I. Wave fields radiated from several types of force systems. J. Phys. Earth, **23**, 205-218.
Sasatani, T., 1984. Synthesis of S-coupled PL waves. J. Fac. Sci. Hokkaido Univ., Ser. 7, **7**, 307-326.
Sato. R., 1969. Formulations of solutions for earthquake source models and some related problems. J. Phys. Earth, **17**, 101-110.
Sato. R., 1973. Seismic waves due to a dislocation source model in a multi-layered medium. Part I. Theory. J. Phys. Earth, **21**, 155-172.
Yao, Z.X. and D.G. Harkrider, 1983. A generalized reflection-transmission coefficient matrix and discrete wavenumber method for synthetic seismograms. Bull. Seism. Soc. Am., **73**, 1685-1699.